Evaluation of EUV resist performance with interference lithography towards 11 nm half-pitch and beyond

Yasin Ekinci (*), Michaela Vockenhuber, Mohamad Hojeij, Li Wang, Nassir Mojarad

Laboratory for Micro- and Nanotechnology, Paul Scherrer Institute, 5232 Villigen PSI, Switzerland;

(*) E-mail: yasin.ekinci@psi.ch; Phone: +41 56 310 2824; Web: http://www.psi.ch/sls/xil

ABSTRACT

The performance of EUV resists is one of the main challenges for the cost-effectiveness and the introduction of EUV lithography into high-volume manufacturing. The EUV interference lithography (EUV-IL) is a simple and powerful technique to print periodic nanostructures with a resolution beyond the capabilities of other tools. In addition, the well-defined and pitch-independent aerial image of the EUV-IL provides further advantages for the analysis of resist performance. In this paper, we present evaluation of chemically-amplified resists (CAR) and inorganic resists using EUV-IL. We illustrate the performance of the tool through a reproducibility study of a baseline resist over the course of 16 months. A comparative study of the performance of different resists is presented with the aim of resolving patterns with CARs for 16 nm half-pitch (HP) and 11 nm HP. Critical dimension (CD) and line-edge roughness (LER) are evaluated as functions of dose for different process conditions. With a CAR with about 10 mJ/cm^2 sensitivity, 18 nm L/S patterns are obtained with low LER and well-resolved patterns are achieved down to 16 nm HP. With another CAR of about 35 mJ/cm^2 sensitivity, L/S patterns with low LER are demonstrated down to 14 nm HP. Resolved patterns are achieved down to 12 HP, demonstrating the capability of its potential towards 11 nm HP if pattern collapse mitigation can be successfully applied. With EUV-sensitive inorganic resists, patterning down to 8 nm has been realized. In summary, we show that resist platforms with reasonable sensitivities are already available for patterning at 16 nm HP, 11 nm HP, and beyond, although there is still significant progress is needed. We also show that with decreasing HP, pattern collapse becomes a crucial issue limiting the resolution and LER. Therefore resist stability, collapse mitigation, and etch resistance are some of the significant problems to be addressed in the development of resist platforms for future technology nodes.

Keywords: EUVL. Extreme Ultraviolet Lithography, interference lithography, photoresist, chemically-amplified resist, CAR, inorganic resist, RLS, LWR, pattern collapse, LER, 16 nm HP, 11 nm HP, single-digit lithography

1. INTRODUCTION

EUV lithography (EUVL) is considered as the leading lithography option for future technology nodes. Among the other challenges, such as source power and mask defectivity, the performance of EUV resists is one of the key factors for the introduction of EUV lithography into high-volume manufacturing. The performance of the resist is defined by the trade-off challenges between the resolution (half-pitch (HP)), sensitivity (dose), and line-edge roughness (LER) [1]. For the future of EUVL, it is crucial to demonstrate the availability and extendibility of the resist paradigms towards further technology nodes, i.e., 16 nm HP, 11 nm HP, and even beyond. Patterning capabilities of different resist platforms have been demonstrated with the present tools for 16 nm HP and beyond [2-4], whereas further optimization is needed, particularly, in LER. In order to ensure timely commercialization of successful resist platforms, development of high-performance (resolution, dose, LER) resists should now address the material solutions towards 11 nm HP.

In this paper, we present performance of different resists using the PSI EUV-IL tool. We focus on resist performance measurements for a range of 22 nm to 7 nm HP with two chemically-amplified resists (CARs) and two inorganic resists. The performance and the long-term reproducibility of our tool are demonstrated using a baseline resist. The results of

Extreme Ultraviolet (EUV) Lithography IV, edited by Patrick P. Naulleau, Proc. of SPIE Vol. 8679, 867910
 · doi: 10.1117/12.2011533

constant monitoring of the tool for the last 1.5 years are presented. A comparative study of the performance of CARs and inorganic resists towards 16 nm HP is discussed. Critical dimension (CD) and LER are evaluated as functions of dose for different process conditions. Moreover, results with CARs down to 12 nm HP are presented, with the aim of resolving patterns with CARs towards 11 nm HP. We also show that with decreasing HP, pattern collapse becomes a crucial issue. For the performance of CARs presented in this paper, we demonstrate that pattern collapse limits the resolution and/or the LER of the resist platforms.

2. PERFORMANCE OF THE EUV-IL TOOL

In interference lithography a periodic aerial image is generated by the interference of two or more coherent beams. EUV-IL setup installed at the Swiss Light Source (SLS), Paul Scherrer Institute, uses transmission and diffraction gratings and spatially coherent EUV light with 13.5 nm wavelength and 4% bandwidth [4]. The masks generally consist of several grating pairs enabling versatile nanostructures or different half-pitches at a single exposure. The aerial image created by interference has infinite depth of focus, i.e., the aerial image is insensitive to variations between the mask and the substrate. Moreover, the aerial image has a period that is half of mask grating for the interference of first-order diffraction beams.

EUV-IL tool at Paul Scherrer Institute is an effective tool for patterning of periodic nanostructures with a resolution beyond the capabilities of other tools. In addition, the well-defined and pitch-independent sinusoidal aerial image of the EUV-IL provides further advantages for the analysis of resist performance [3-6]. The performance of the tool has been steadily improved during the last 10 years and has been always the leading tool in terms of resolution. With this tool 12.5 nm HP, 11 nm HP, 8 nm HP resolutions were demonstrated in 2007, 2009, 2012, respectively [4, 7, 8]. Relative simplicity of EUV-IL and its low-cost compared to high-NA projection tools, make it a promising alternative for resist testing for future technology nodes as well as for academic research where high-resolution nanostructures are needed.

We are monitoring the long-term performance and the stability of the tool with a baseline resist. Figure 1 shows the dose-dependent CD and LER of Resist-A for the exposures performed within a time interval of 16 months. We note that we did not exclude any outlier data in this figure. We used the same mask, beam conditions, and resist processing parameters, which are listed in Table 2 in the next Section. In all experimental runs, high quality patterns were obtained. Exposures were performed with 4 resist batches, which were replaced after 6 months of shelf storage. We did not see any significant change in the resist performance and sensitivity during these experiments, demonstrating the excellent shelf life of the resist.

In Figure 2, obtained dose-to-size values leading to 1:1 L/S patterns at different HPs for all experimental runs are plotted. The variations in the CD and LER results partly from the analysis of the SEM images where we obtain certain error bands that are not provided here. In addition, there are several possible sources for errors. The SEM inspection of the samples is done by a multipurpose SEM. Therefore, the obtained CD and LER values are subject to change depending on the SEM settings and condition, although we try to keep the settings constant for our purpose. Moreover, tool stability and human factor also play a significant role. Minor changes in the illumination optics, diode aging and its recalibration, and other tool-related factors that may cause these variations.

As seen in Figure 2, we do not see any trend of change in the dose-to-size of the resist within the variations of the long-term data. In comparison of the variations between different half-pitches for an individual experiment, we see both correlated and uncorrelated variations. Correlated variations result from the changes in the exposure tool and SEM inspection whereas uncorrelated variations are due to other factors such as statistical errors in analysis.

The results presented in Figures 1 and 2 are summarized in Table-1. The dose-to-size values that are averaged over all experiments are provided for different half-pitches. In addition to the standard deviation of measurements, a 10% error should be added to the absolute dose-to-size values due to the possible errors in tool factor measurements. During the exposures we measure the dose-on-mask, which is converted to dose-on-wafer using predetermined tool factors. The tool factors, which are obtained experimentally, account for the diffraction efficiency and the transmission of the masks. The method of extracting the tool factors, which is described elsewhere [4], has an error of about 10%.

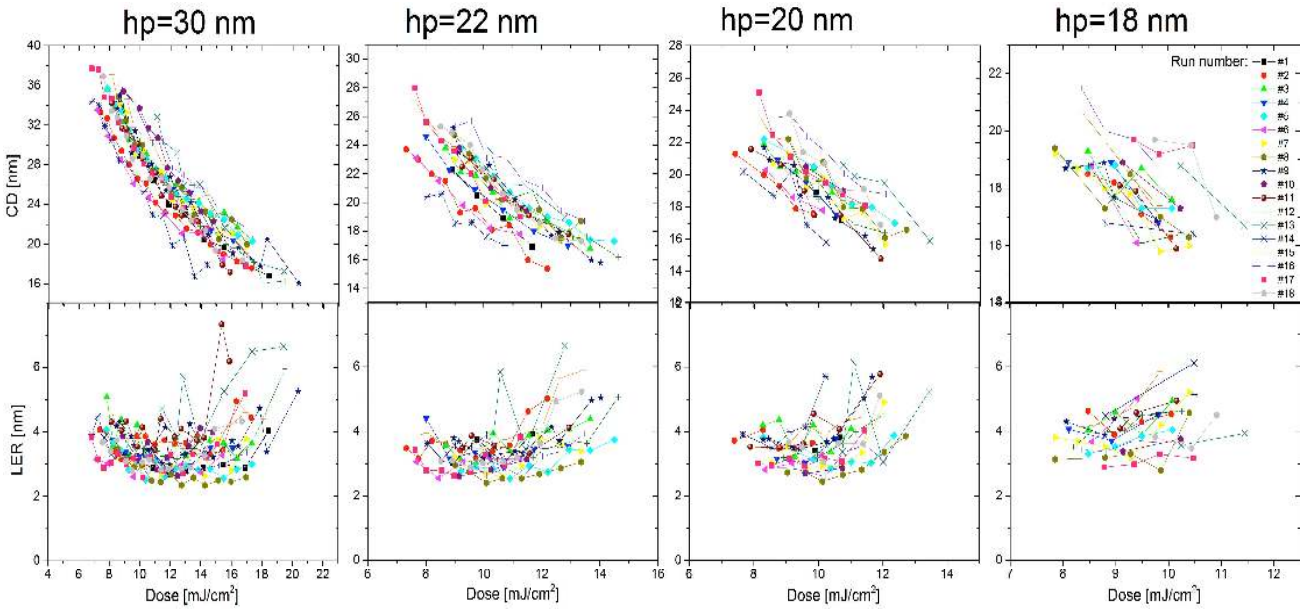

Figure 1. CD and LER of Resist-A as functions of dose at different half-pitches for experiments performed in the course of 16 months. Information on Resist-A is provided in Table 2.

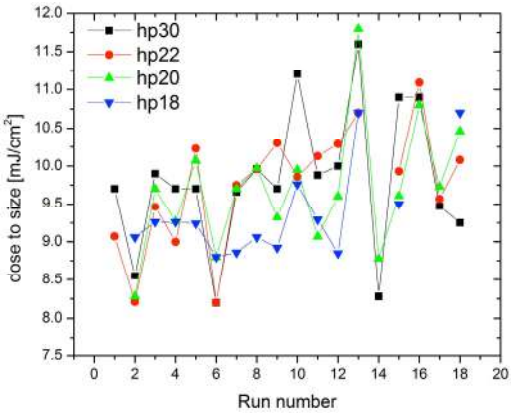

Figure 2. Variations of dose-to-size (L/S=1:1) at different half-pitches for all the experimental runs performed in the course of 16 months with the baseline resist. The data is obtained from the analysis of Figure 1.

Table 1. Summary of the results shown in Figs.1 and 2. Average dose and standard deviation (σ) denote the mean value and variation of all experimental runs. Systematic error accounts for the possible sources of errors in the dose calibration and determination of tool factors, which is estimated as 10%.

In mJ/cm^2	**HP 30 nm**	**HP 22 nm**	**HP 20 nm**	**HP 18 nm**
Average dose-to-size	9.80	9.65	9.71	9.51
Standard deviation	0.94	0.87	0.79	0.67
Systematic error	0.98	0.97	0.97	0.95

3. COMPARATIVE STUDY OF RESISTS TOWARDS 16 NM HP

In this section we present the performance of CARs and inorganic resists for half-pitches between 22 nm and 16 nm. For the resist characterization, L/S patterns with 22 nm, 20 nm, 18 nm, and 16 nm HPs were exposed with the same mask. The patterns were analyzed with top-down SEM images that were captured at the same magnification and with an acceleration voltage of 1 kV in order to minimize the effect of the SEM inspection. The analysis of the CD and LER values were performed with a commercial analysis and modeling software (SuMMIT ®). LER values correspond to 3σ deviation after a certain frequency filtering.

The resists that are evaluated in this study and their processing parameters are listed in Table-2. In addition to two CARs with positive tone, we have evaluated 4 different inorganic resists with negative tone. Hafnium-based inorganic resists (Inpria) have two formulations of high sensitivity (Inpria/JB) and high resolution (Inpria/IB). These resists show very good performance with relatively low dose [4, 9]. Hydrogen silsesquioxane (HSQ) is a silicon-based resist, which is well known for its high-resolution in academic research, but requires very high dose for EUV patterning [4, 10]. Although there are two HSQ resists listed in Table-2, both have the same formulation but differ in development. Dose-to-clear curves for these resists are shown in Fig. 3. Obtained values of dose for 50% clearance are listed in Table-2. These values are obtained by best-fit parameters to the curves in Fig. 3 using the function

$$t(D) = t_0[1 + 10^{(LogD_0 - D)\cdot p}]^{-1} \quad (1)$$

where, D is the dose, t_0 is the maximum thickness difference of unexposed or overexposed resist, $Log\ D_0$ is the dose for 50% clearance and p is the slope, i.e. contrast. We found this equation, which is called as dose response function in pharmaceutical sciences, very effective, since it does not rely on arbitrary clearance thresholds and is very robust to low-sampled data. We note that the present inorganic resists show some aging effects in sensitivity and resolution and therefore the reported sensitivities can differ. For instance, the effect of aging on sensitivity is shown for HSQ in Fig. 3.

Table 2. Process parameters and sensitivities of the resists used in this study. Dose-to-clear denotes 50% thickness loss after open-frame EUV exposure. It should be noted that the sensitivities of inorganic resists (listed in the last column) may change during the shelf life.

Resist name	Supplier	Substrate	Spinning	PAB	Thickness	PEB	Developer / Time	Sensitivity mJ/cm^2
Resist-A	Shin-Etsu	Si/Underlayer	2500 rpm / 45s	105°C / 90s	35 nm	90°C / 90s	TMAH 0.26N / 30s	4.5
Resist-B	JSR	Si/Underlayer	2500 rpm / 60s	130°C / 60s	30 nm	110°C / 60s	TMAH 0.26N / 30s	15
Inpria/XE15JB	Inpria	Si/O_2 Plasma	2500 rpm / 45s	80°C / 120s	20 nm	80°C / 120s	TMAH 25% /120s	25
Inpria/XE15IB	Inpria	Si/O_2 Plasma	2500 rpm / 45s	80°C / 180s	20 nm	80°C / 60s	TMAH 25% /30s	47
HSQ/TMAH	Dow Chem.	Si	5000 rpm / 45s	No	35 nm	No	TMAH 2.6N / 60 s	82
HSQ/351	Dow Chem.	Si	5000 rpm / 45s	No	35 nm	No	351 /30 s	294

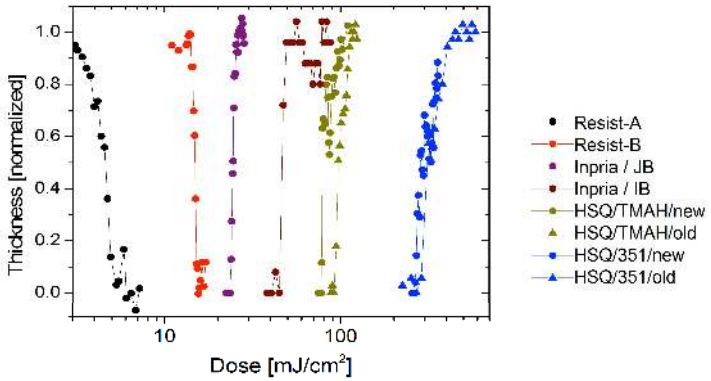

Figure 3. Dose-to-clear curves of CARs and inorganic resists. Process conditions of the resists are provided in Table 2. New and old for HSQ refer to fresh and 6-month-old resist batches, respectively.

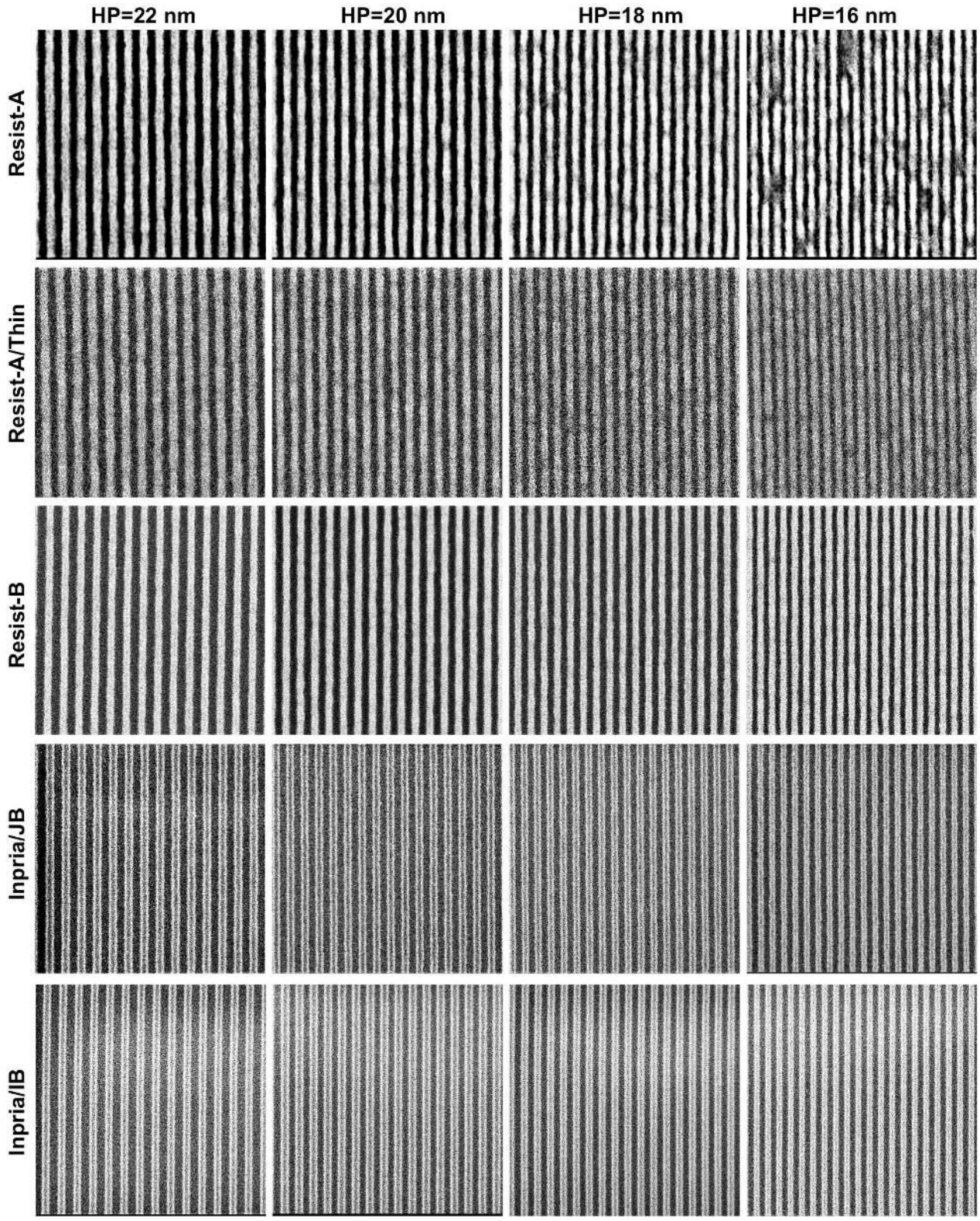

Figure 4. SEM images of CARs and inorganic resists at different half-pitches. Process conditions of the resists are provided in Table 2. Resist-A/Thin has a thickness of 30 nm instead of 35 nm.

Figure 4 shows the SEM images of different resists at optimal doses at half-pitches of 22 nm to 16 nm. In this figure data for HSQ resist is not shown and can be found elsewhere [4]. All the resists with the exception of Resist-A show well-resolved patterning down to 16 nm HP. For Resist-A, patterns are resolved down to 18 nm HP. For half-pitch of 16 nm pattern collapse appears as the major problem. Although there are many effective pattern mitigation methods are available, as the most straightforward way, we reduced the resist thickness from 35 nm to 30 nm. In this case, the SEM images referring to Resist-A/Thin are obtained, showing increased LER and significant necking. Quantitative LER values were reported in a previous publication [4]. It should be noted that the initial resist thickness was already reduced to 35 nm instead of commonly used thickness of 40 nm. Resist-A is clearly a high-performance resist with a well-balanced trade-off between resolution, LER, and dose. A resolution of 18 nm HP with reasonable LER and sensitivity of 10 mJ/cm^2 is obtained. In addition, well-resolved patterns with 16 nm HP can be achieved with about the same dose and with significantly high LER. The use of thinner resist as a pattern collapse mitigation is obviously not an effective method because it increases the LER significantly. These results show that 16 nm HP with 10 mJ/cm^2 sensitivity can be achieved with further improvements, in particular with effective collapse mitigation methods.

As seen in SEM images in Fig. 4, Resist-B exhibits excellent performance down to 16 nm HP. Through-dose dependences of CD and LER for this resist are shown in in Fig. 5. In order to check the reproducibility of the resists, the experiment is repeated within a time interval of several months. The LER values as low as 2 nm have been achieved for all half-pitches. The dose-to-size at all half-pitches is about 30-35 mJ/cm^2. Since interference lithography creates a pitch-independent aerial image, dose-to-size is also independent for an ideal image and should be equivalent to twice the dose-to-clear. For Resist-B, the results are very close to this ideal case.

Figure 6 shows the CD and LER functions of dose for selected resists at 16 nm HP. We included Resist-A with reduced thickness, Resist-B, and Inpria/JB. Although other resists that are not shown in the figure but listed in Table-2 show very low LER, they are not considered for this resolution because of their unnecessarily high dose-to-size. This figure gives an overview of the available resist platforms for 16 nm HP. A comparison of LER values of the different resists for the same half-pitch reveals a clear correlation between LER and the sensitivity. For patterning at 16 nm HP, Resist-B would be the most obvious option considering both LER and sensitivity. Although Resist-A has very large LER in this figure, there is a significant potential of improvement with this resist platform. Pattern collapse mitigation methods will enable to pattern the same resist with a thickness more than 30 nm and thereby will lead to significant reduction in LER. Alternatively, modifications in resist's formulation or further optimization of the processing parameters leading to slightly reduced sensitivity might enable patterning with low LER at 16 nm HP.

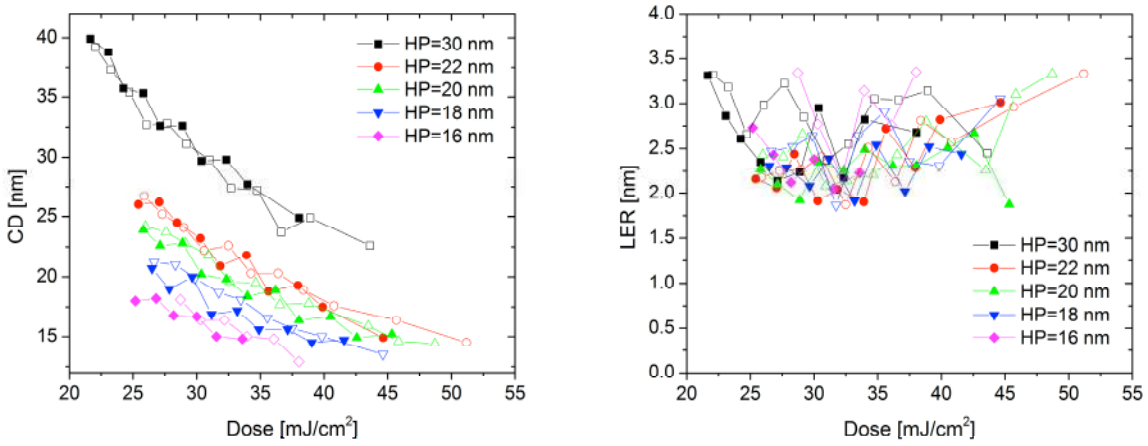

Figure 5. CD and LER of Resist-B as functions of dose at 30 nm to 16 nm HPs. Details on the resist and its process parameters are provided in Table-2. Filled and unfilled symbols stand for two independent experiments run at different times.

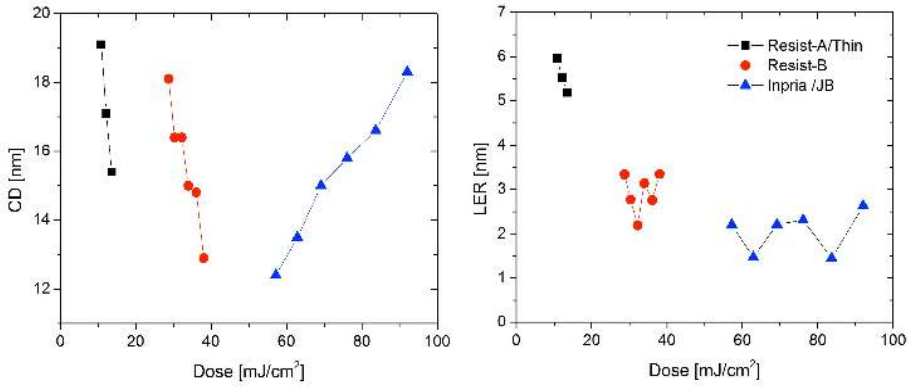

Fig 6. CD vs. dose and LER vs. dose curves for selected resists at 16 nm HP. Details on resists can be found in Table-2 whereas Resist-A/Thin refers to with the only difference in thickness which is 30 nm.

4. EVALUATION OF EUV RESISTS TOWARDS 11 NM HP

As discussed in Section 3, Resist-B and all the inorganic resists evaluated in this study show low LERs down to 16 nm HP. Certainly, the ultimate resolution of these resists should reach beyond 16 nm HP. In this section, evaluation of these resists in the sub-16 nm range is presented with the aim of exploring their performance towards 11 nm HP. Figure 7 shows the SEM images of Resist-B for half-pitches 15 nm to 12 nm. With the standard processing conditions of Resist-B, well-resolved patterns down to 15 nm HP are obtained and beyond this resolution significant pattern collapse is observed. In order to reduce the pattern collapse, the resist thickness is reduced from 30 nm to 25 nm. In this case, as denoted Resist-B/Thin in Fig. 7, well-resolved patterns down to 14 nm HP, and resolved patterns with partial collapse down to 12 nm have been achieved.

In Figs. 8 and 9, the dose dependences of CD and LER for Resist-B with standard thickness and reduced thickness are presented, respectively. Exposure latitude decreases with decreasing half-pitch. As can be inferred from the figures, for the thick resist the LER values at different half-pitches remain in the range of 2 nm to 2.5 nm, whereas for the thin resist the LER values increase to a value of about 3.5 nm. As it was observed for Resist-A, reduction of the resist thickness leads to increase in LER and the resist thickness should not be less than 30 nm.

The dose-to-size values for all HPs are in the range of 35-42 mJ/cm^2. These values are slightly higher than the values reported in the previous section. A comparison between Figs. 5 and 8 reveals that the dose values for the same half-pitches differ in these figures, although the resist formulation and its processing are the same. The difference between these figures is due to the error in the determination of the tool factors. The results in Fig. 5 and Fig. 8 are obtained using two different masks. As mentioned in the Section 2, there is a certain error in the measuring the tool factors and once a tool factor is obtained and used this leads to a systematic error in dose values reported. Repetitive measurements of the tool factors revealed that the accuracy of the tool factors is about 10%.

As of submission date of this manuscript, we have not tested any CAR that can achieve 11 nm HP resolution. Nevertheless, Resist-B or its optimized formulations hold the promise for 11 nm HP. Currently, only inorganic resists can achieve this challenging target. As we mentioned, among the inorganic resists, the resist platform of Inpria has the highest resolution with reasonable sensitivity. In Fig. 10, the SEM images of high-resolution patterning with Inpria/JB and Inpria/IB are shown, where patterns with 12 nm HP and 8 nm HP are obtained, respectively. Although we have not obtained the dose on mask at these HPs yet, we take the liberty of extrapolating the dose-to-size values obtained at higher half-pitches. In the range of 30 nm to 16 nm, we measured dose-to-size values of 75-80 mJ/cm^2 and 160-200 mJ/cm^2 for Inpria/JB and Inpria/IB, respectively. As we mentioned in the previous sections, the aerial image of interference lithography is, in principle, pitch-independent. We have observed in the results presented in this work and previous works [4] that for all resists the dose-to-size is relatively independent of half-pitch within range of 30 nm to 12 nm HP. We predict that the dose-to-size values should not be significantly different at lower half-pitches.

HSQ also has superior performance in terms of resolution, however it is a slow resist due to the low absorption of Si at EUV wavelength. Last year we have reported 8 nm HP resolution with HSQ resist. Recently, we have achieved well-

resolved patterns at 7 nm HP. The details will be published elsewhere. This shows that we are steadily making progress with holographic patterning and there is still a lot of room for further improvement. This record resolution was enabled by the use of Inpria resists for mask fabrication. High-resolution e-beam lithography with this resist platform and its EUV efficiency provides significant advantages for the fabrication of diffractive EUV optics with high quality and efficiency.

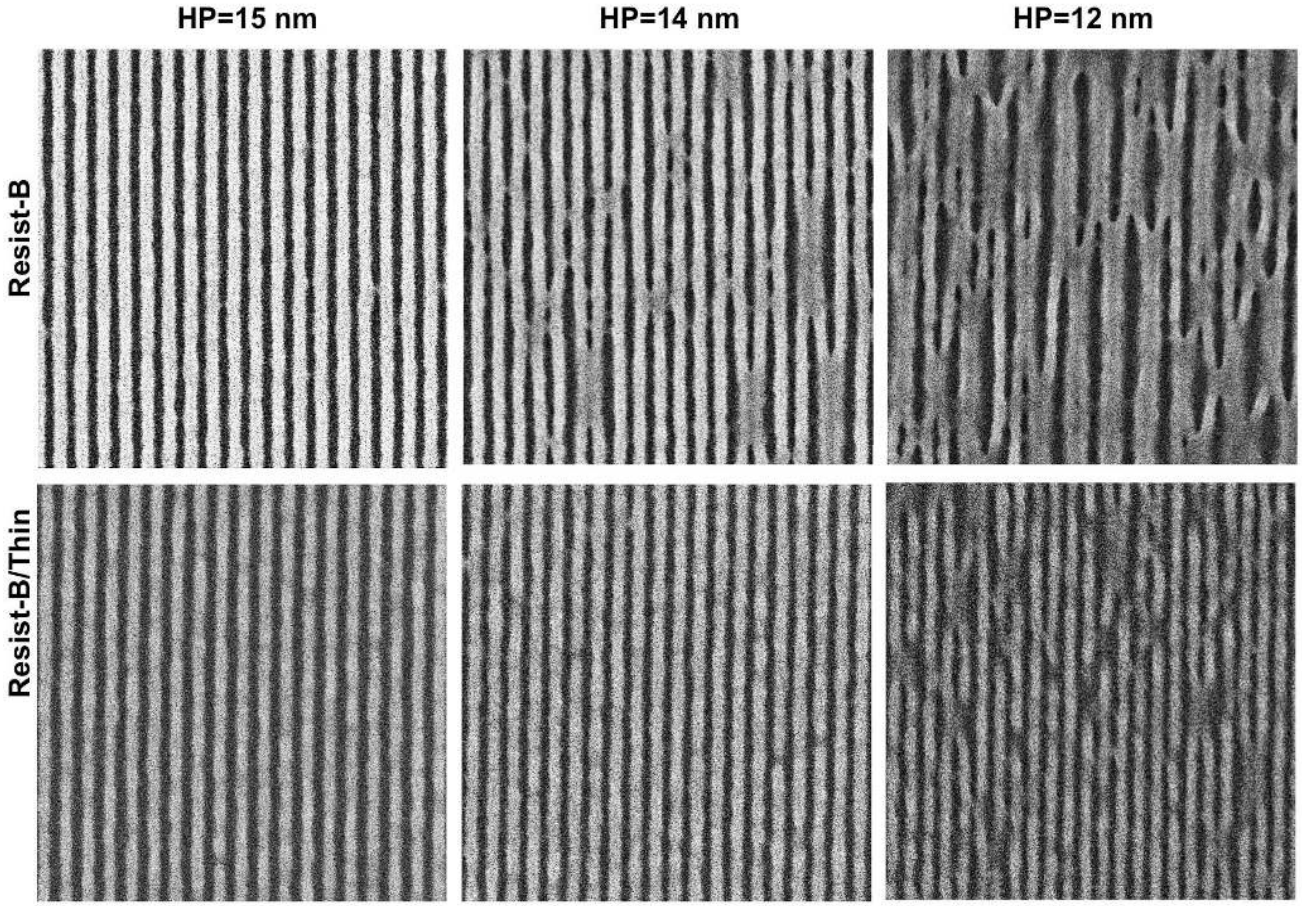

Figure 7. SEM images of CARs and inorganic resists at different half-pitches. Process parameters are provided in Table 2. Resist-B/Thin refers to resist thickness of 25 nm instead of the standard thickness of 30 nm.

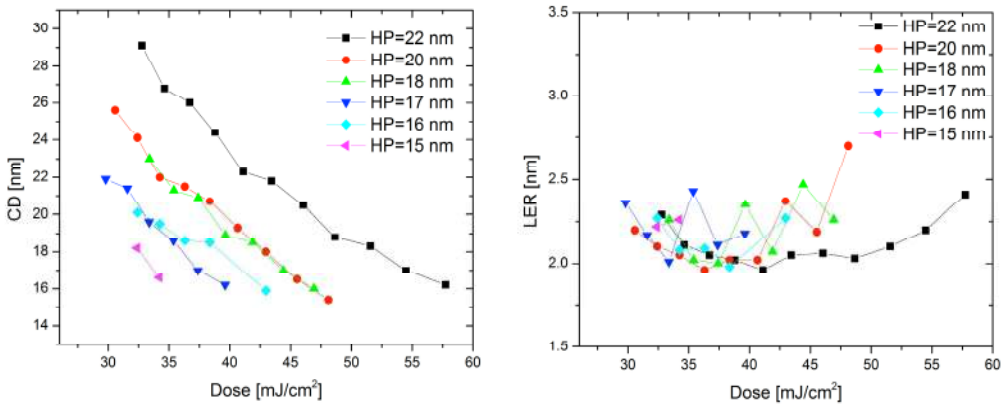

Figure 8. Through-dose behavior of CD and LER of Resist-B at 22 nm to 15 nm HPs. Process parameters are provided in Table 2.

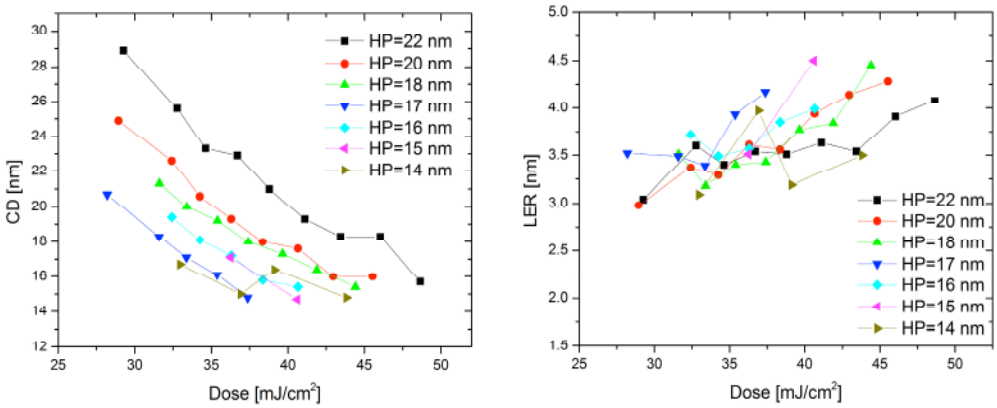

Figure 9. Through-dose behavior of CD and LER of Resist-B at 22 nm to 15 nm HPs. Process parameters are provided in Table 2 with a difference of spinning at higher speed resulting in a resist thickness of 25 nm.

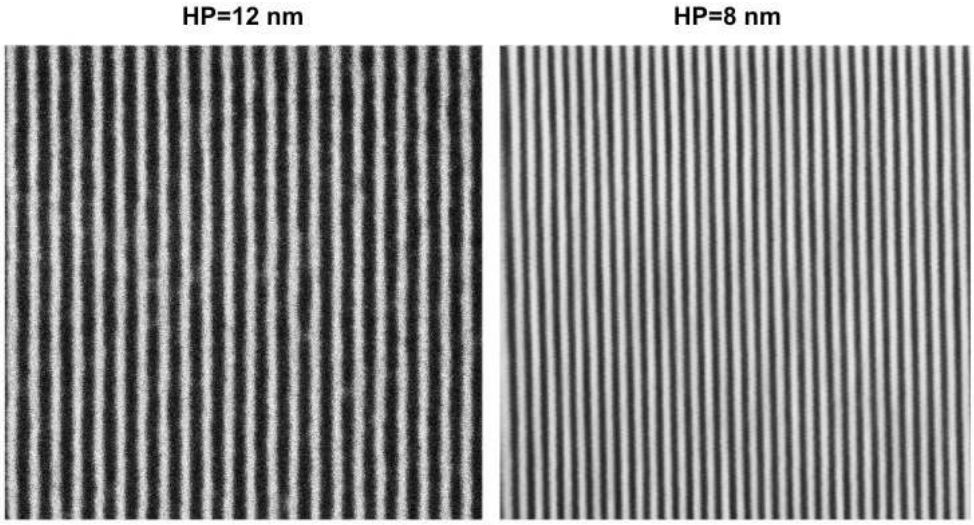

Figure 10. Top-down SEM images of the highest resolutions obtained with EUV-sensitive inorganic resists. Left: 12 nm HP L/S patterns with Inpria/JB (high-sensitivity) resist. Right 8 nm HP L/S patterns with Inpria/IB (high-resolution) resist. Process parameters are provided in Table 2. For 8 nm HP, the resist thickness was reduced below 15 nm.

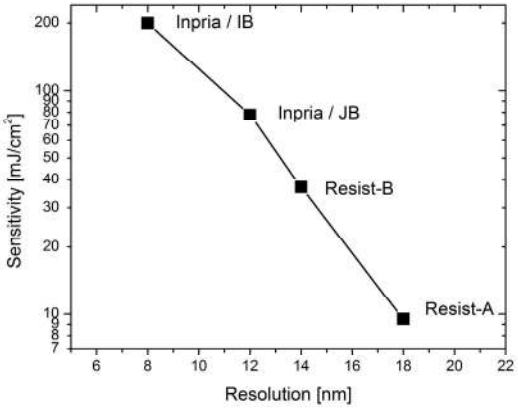

Figure 11. Sensitivity vs. resolution for the champion resists. Resolution denotes the highest resolution achieved currently. Sensitivity denotes the measured or estimated dose-to-size at the given HP.

An overview of the performances of the evaluated resists in this study is shown in Fig. 11 wherein the highest achieved resolutions and dose-to-size values of individual resists are plotted. This figure illustrates the state of the art in simplistic way, although the true performance should be a 3D plot in dose-resolution-LER parameter space. This figure is a culmination of the results presented above where patterns with 18 nm HP are obtained with Resist-A and with 14 nm half-pitch are obtained with Resist-B as well as 12 nm HP and 8 nm HP resolutions are obtained with high-sensitivity and high-resolution Inpria resists, respectively. Interestingly, the logarithm of the sensitivity linearly scales with the resolution.

5. CONCLUSIONS

The results of the monitoring the performance of the PSI's tool with a baseline CAR are presented, demonstrating the excellent long-term performance and stability of the tool. CARs and inorganic resists are evaluated in the sub-22 nm regime with the aim of evaluating the availability of the resist for 16 nm HP, 11 nm HP resolution and for generations beyond 11 nm HP. CD and LER are evaluated as functions of dose for different CARs and inorganic resists in the range of 22 nm to 11 nm HP.

These results demonstrate that EUV-IL is a powerful and simple method for evaluation of EUV resist performance for future technology nodes, helping to fill the time gap until high-NA scanners are realized. The timely development of the material solutions, illustrating the extendibility of resist paradigms, and demonstrating the feasibility of patterning at future technology nodes are strategically important for the future of EUVL.

We have shown that EUV photons can resolve down to 7 nm HP, demonstrating the proof of concept that there are no fundamental limitations in terms of photochemistry and materials science. It can be concluded from these results that secondary electron blur in EUV lithography will not be a limiting factor for 16 and 11 nm HPs or even below. Indeed, we are optimistic that our performance in ultimate resolution can be improved further. In the last 10 years, the resolution of PSI's tool has improved steadily with a rate of 1 nm/year. We believe that there is still some room for further progress in resolution, whereas the ultimate fundamental limit is about 3.5 nm HP.

The comparative study of the CARs showed that the current status of the EUV resist development is very promising and highly advanced. CAR platforms are already available for 22 nm HP and 16 nm HP. Moreover, for 11 nm HP, CARs might be feasible with further developments. The current status shows an increasing dose with decreasing HP as shown in Fig. 11. This is an expected result, based on the fundamental effects of shot noise and acid diffusion blur, although the dependence of dose and resolution due to these effects can be somewhat different [11]. Nevertheless, the trend illustrated in Fig. 11, in which going from 22 nm to 16 nm, and to 11 nm HP, resists get slower and thinner, will be valid also in future, and therefore target sensitivity specifications should be realistic values. Surprisingly, the champion resists with different formulations and with and without chemical amplification, lie along the same line as shown in Fig. 11. Detailed stochastic simulations can provide further insight as well as can give and estimation of the potential of development towards the absolute theoretical limit of sensitivity vs. resolution.

The measure of progress in EUV resist development for 16 nm and 11 nm nodes is set by the sensitivities of these available platforms. The dose and resolution curve in Fig. 11 illustrates the current status of resist development. Future developments should aim for either decreasing the HP with the same dose or decreasing the dose for the target HP, thereby shifting the curve towards lower dose and HP. Future development for 16 nm HP should be towards faster CAR than the available materials without any significant compromise in resolution. For 11 nm HP, slower CARs and faster inorganic resists may provide the resolution and LER with maximum sensitivity.

With decreasing HP, pattern collapse becomes the limiting factor. We note that for all the resists presented in this study, either the resolution is limited by pattern collapse (CARs) or it was the major problem to overcome (inorganic resists). There is a clear correlation between the LER and resist thickness. For instance, for Resist-A, resist thickness should be at least 35 nm and, if possible even more, through collapse mitigation strategies. If this can be achieved, it might be possible to have a resist with a sensitivity of 10 mJ/cm^2 at 16 nm HP. Similarly, Resist-B may provide 12 nm HP resolution or eventually 11 nm HP resolution with a sensitivity of 35 mJ/cm^2. This seems to be also the case for the inorganic resists, which are relatively thin and are known for their great stability. Therefore, successful pattern collapse mitigation strategies can shift the curve in Fig.11 by a few nm in resolution without any change in the material processing. Further progress should, therefore, include pattern collapse mitigation techniques, such as super-critical drying or special development recipes like FIRM^{TM} [12, 13].

ACKNOWLEGMENTS

We are grateful to Markus Kropf for his technical assistance, to Inpria Corp., Shin-Etsu, and JSR for providing the resists, to Todd R. Younkin for indispensible discussions. Part of this work was performed at Swiss Light Source (SLS), Paul Scherrer Institute.

REFERENCES

[1] Putna, E. S., Younkin, T. R., Leeson, M., Caudillo, R., Bacuita, T., Shah, U. and Chandhok, M., "EUV lithography for 22 nm half pitch and beyond: Exploring resolution, LWR, and sensitivity tradeoffs," Proc. SPIE 7969, 79692K (2011).

[2] Anderson, C., Ashworth, D., Baclea-An, L. M., Bhattari, S., Chao, R., Claus R., Denham, P., Goldberg, K., Grenville, A., Jones, G., Miyakawa, R., Murayama, K., Nakagawa, H., Rekawa, S. and Stowers, S., "The SEMATECH Berkeley MET: demonstration of 15-nm half-pitch in chemically amplified EUV resist and sensitivity of EUV resists at 6.x-nm," Proc. SPIE 8322, 832212 (2012).

[3] Ongayi, O., Christianson, M., Meyer, M., Coley, S., Valeri, D., Amy, K., Wagner, M., Cameron, J. and Thackeray, J., "High sensitivity chemically amplified EUV resists through enhanced EUV absorption," Proc. SPIE 8322, 83220T (2012).

[4] Ekinci, Y., Vockenhuber, M., Terhalle, B., Hojeij, M., Wang L. and Younkin, T. R., "Evaluation of resist performance with EUV interference lithography for sub-22 nm patterning," Proc. SPIE 8322, 83220W (2012).

[5] Gronheid, R., Solak, H. H., Ekinci, Y., Jouve, A. and Van Roey, F., "Characterization of extreme ultraviolet resists with interference lithography," Microelectron. Eng. 67-68, 1103 (2006).

[6] Goethals, A. M, Gronheid, R., Van Roey, F., Solak, H. H. and Ekinci, Y., "Progress in EUV resist performance," J. Photopolymer Sci.& Tech. 19, 501 (2006).

[7] Solak, H. H., Ekinci, Y., Käser. P. and Park, S., "Photon-beam lithography reaches 12.5 nm half-pitch resolution," J. Vac. Sci. Technol. B 25, 91 (2007).

[8] Päivänranta, B., Langner, A., Kirk, E., David, C. and Ekinci, Y., "Sub-10 nm patterning using EUV interference lithography," Nanotechnology 22, 375302 (2011).

[9] Stowers, J. K., Telecky, A., Kocsis, M., Clark, B. L., Keszler, D. A., Grenville, A., Anderson, C. N. and Naulleau, P. P., "Directly patterned inorganic hardmask for EUV lithography," Proc. SPIE 7969, 796915 (2010).

[10] Ekinci, Y., Solak, H. H., C. Padeste, C., Gobrecht, J., Stoykovich, M. P. and Nealey, P. F., "20 nm Line/Space Patterns in HSQ Fabricated by EUV Interference Lithography," Microelectron. Eng. 84, 700 (2007).

[11] Naulleau, P. P., Anderson, C. N., Baclea-an, L-M., Denham, P., George, S., Goldberg, K. A., Jones, G., McClinton, B., Miyakawa, R., Rekawa, S. and Smith, N., "Critical challenges for EUV resist materials," Proc. SPIE 7972, 797202 (2011).

[12] Goldfarb, D. L., Bruce, R. L., Bucchignano, J. J., Klaus, D. P., Guillorn, M. A. and Wu, C. J., "Pattern collapse mitigation strategies for EUV lithography," Proc. SPIE 8322, 832205 (2012).

[13] Shite, H, Bradon, N., Shimoaoki, T., Kobayashi, S., Nafus, K., Kosugi H., Foubert, P., Hermans J., Hendrickx, E., M. Goethals, M., R. Gronheid, R. and Jehoul, C., "EUV processing investigation on state of the art coater/developer system," Proc. SPIE 7969, 796937 (2011).